Mon. Not. R. Astron. Soc. **267**, 303–311 (1994)

On the polarization of resonantly scattered emission lines – I. Emission and absorption coefficients in an anisotropic radiation field

H.-W. Lee,[1] R. D. Blandford[1] and L. Western[2]

[1] *Theoretical Astrophysics 130-33, California Institute of Technology, Pasadena, CA 91125, USA*
[2] *Aerospace Corporation, El Segundo, Los Angeles, CA 90061, USA*

Accepted 1993 October 14. Received 1993 August 24; in original form 1993 June 23

ABSTRACT

Source functions and absorption coefficients for polarized radiation in a given anisotropic radiation field are calculated for a variety of permitted electric dipole transitions in the L–S coupling limit. Collisional, radiative and magnetic mixing of the ground sublevels are all considered. The polarization of the self-consistent, emergent radiation field is computed, using an anisotropic escape probability formalism to treat the radiative transfer. It is found that the radiative mixing can enhance the polarization for transitions with large angular momentum, and degrees of polarization $\lesssim 10$ per cent are obtained for transitions with small angular momentum.

Key words: atomic processes – line: formation – polarization – radiative transfer – galaxies: active.

1 INTRODUCTION

Recent developments in spectropolarimetry have made possible the measurement of the linear polarization of broad emission lines in active galactic nuclei (AGN) with accuracies ~0.3 per cent (e.g. Goodrich 1991; Netzer 1990). Such measurements provide a possible probe of the hitherto uncertain distribution of emission (and absorption)-line gas in phase space. This motivates calculations of the degree of linear polarization to be expected from simple source models involving an aggregation of discrete clouds. Somewhat unfamiliar physical principles are involved, however, and it is the purpose of this paper to elucidate them.

Most of the spectral lines of interest involve ground-state, electric dipole transitions in which a photon is created following an electron collisional excitation. This photon scatters many times off other ions within the same cloud until its Doppler shift is large enough to allow it to escape. Spatial transport within the cloud and scattering by other clouds is relatively unimportant in most simple cases. If the radiation field is isotropic, polarization of the emergent radiation field should not develop. However, these clouds, which are popularly supposed to be moving with Mach numbers in excess of 1000, are likely to have significant internal velocity shears, and this will cause photon escape to be anisotropic. Under these conditions, polarization, roughly proportional to the anisotropy in the radiation field, should be observed.

In Section 2, we describe the atomic physics relevant to the computation of the degree of polarization from resonant line scattering. We calculate the absorption coefficient and source function for radiation with an arbitrary distribution in polarization and angle and a variety of permitted transitions. In this section, it is assumed that collisions populate the ground substates equally. In Section 3, we relax this assumption, and instead assume that radiative excitation is more frequent than collisional excitation, as indeed is likely to be the case for strong permitted lines in an AGN emission-line cloud. We show that the ground sublevels will now be unequally populated in the steady state and that the polarizing effect will mostly be enhanced. A further complicating effect involves the magnetic field. If the electron–cyclotron frequency significantly exceeds the radiative excitation rate or, for semiforbidden lines, the Einstein A coefficient, then either the ground or the excited state sublevels can be mixed so that they are effectively resolved into eigenstates of the magnetic perturbation operator. A field of no more than ~0.01 G may be all that is necessary for this effect to be important. Magnetic fields of larger strength have been invoked in some broad-emission-line region models (e.g. Emmering, Blandford & Shlosman 1992). This is discussed in Section 4. In Section 5 we apply our result to a calculation of the polarization of the escaping radiation assuming a frequency- and polarization-independent but angle-dependent escape probability. This can be used in simple estimates of the magnitude of the emergent polarization. Our conclusions are briefly collected in Section 6.

In Paper II, we shall use this formalism in Monte Carlo calculations of radiative transfer in model emission-line clouds. These calculations do not assume the complete frequency redistribution that was adopted in Section 5 of this paper. We shall also consider spatial transport under conditions of reduced optical depth appropriate to the semi-

forbidden emission lines. In Paper III, we will then consider global models of AGN broad-emission- and absorption-line clouds and compute the predicted degree of linear polarization from spatially unresolved observations.

2 EMISSION AND ABSORPTION COEFFICIENTS – COLLISIONAL MIXING

Consider an ion described in the Russell–Saunders (L–S coupling) approximation. The ground state is characterized by combined spin S, orbital angular momentum L and total angular momentum J quantum numbers. In permitted, electric dipole transitions, the selection rules $\Delta S=0$, $\Delta L=0$, ±1, $\Delta J=0$, ±1 ($0\rightarrow0$ forbidden) operate. Let the subscript g denote the ground state and the subscript e the excited state. The ground and excited states have $2J_{g,e}+1$ degenerate sublevels labelled by additional quantum numbers $M_{g,e}\equiv g, e$ varying between $-J_{g,e}$ and $J_{g,e}$. Transitions between sublevels of the ground and the excited states are limited by the selection rule $\Delta M=e-g=0$, ±1 ($0\rightarrow0$ forbidden for $\Delta J=0$).

Using standard, time-dependent perturbation theory (e.g. Merzbacher 1961), it can be shown that a pulse of polarized radiation will induce a transition of the ion from an initial, pure ground state $|g\rangle$ to an excited, final state expanded in terms of orthonormal eigenfunctions $|e\rangle$ as $|e\rangle c_e$, where the coefficient is

$$c_e=\frac{-\mathrm{i}|e|}{\hbar}\langle e|\boldsymbol{x}\cdot\tilde{\boldsymbol{E}}|g\rangle, \tag{2.1}$$

where $\tilde{\boldsymbol{E}}=\tilde{E}_q\boldsymbol{e}_q$ is the Fourier transform of the wave electric vector and $|e|$ is the electronic charge. (In this paper we sum implicitly over repeated indices unless explicit summations are given.) The coefficient c_e is assumed to be much less than unity.

Without loss of generality, we choose a particular set of Cartesian coordinates (x, y, z) and expand the sublevels in eigenstates of J_z. We shall also use standard spherical polar coordinates (r, θ, ϕ). The electric vector is then conveniently expanded in an orthonormal basis with (ion) basis vectors $\boldsymbol{e}_q$:

$$\begin{aligned}\boldsymbol{e}_-&=2^{-1/2}(\hat{\boldsymbol{x}}-\mathrm{i}\hat{\boldsymbol{y}}),\\ \boldsymbol{e}_0&=\hat{\boldsymbol{z}},\\ \boldsymbol{e}_+&=2^{-1/2}(-\hat{\boldsymbol{x}}-\mathrm{i}\hat{\boldsymbol{y}}).\end{aligned} \tag{2.2}$$

For the ingoing and outgoing photon states, however, we use a two-component (photon) basis $\boldsymbol{e}_\alpha$, comprising $\boldsymbol{e}_\parallel$ which lies in the $\boldsymbol{n}$–$\hat{\boldsymbol{z}}$ plane, where $\boldsymbol{n}$ is the direction of wave propagation, and $\boldsymbol{e}_\perp$ which is in the direction $\boldsymbol{n}\times\hat{\boldsymbol{z}}$. (See Fig. 1.)

We define a 2×3 matrix, $S_{\alpha q}$, to transform from the ion basis to the photon basis associated with a particular direction $\boldsymbol{n}$:

$$\boldsymbol{e}_\alpha=S_{\alpha q}\boldsymbol{e}_q, \tag{2.3}$$

$$S_{\alpha q}=\begin{pmatrix}2^{-1/2}\cos\theta\mathrm{e}^{\mathrm{i}\phi} & -\sin\theta & -2^{-1/2}\cos\theta\mathrm{e}^{-\mathrm{i}\phi}\\ 2^{-1/2}\mathrm{i}\mathrm{e}^{\mathrm{i}\phi} & 0 & 2^{-1/2}\mathrm{i}\mathrm{e}^{-\mathrm{i}\phi}\end{pmatrix}. \tag{2.4}$$

The spontaneous transition rate $\mathrm{d}\dot{P}$ from the excited state $|e\rangle$ to the ground state $|g\rangle$, which creates a photon in polarization $\boldsymbol{e}_\alpha$ that propagates along a direction lying in $\mathrm{d}\Omega$, can be written

$$\mathrm{d}\dot{P}=A|M_{eg}(\boldsymbol{e}_\alpha)|^2\,\mathrm{d}\Omega, \tag{2.5}$$

where A is the total Einstein A coefficient from an excited state and $M_{eg}(\boldsymbol{e}_\alpha)$ is proportional to the matrix element for the transition. We can write

$$M_{eg}(\boldsymbol{e}_\alpha)=S_{\alpha q}R^q_{eg}, \tag{2.6}$$

where R^q_{eg} is a (normalized) Clebsch–Gordan coefficient for an angular momentum change of unity and $q=e-g=0$, ±1 for an electric dipole transition. According to the Wigner–Eckart theorem, the Einstein A coefficient depends just on J_g, J_e (e.g. Merzbacher 1961). The Clebsch–Gordan coefficients can be written in terms of the quantum numbers of the excited state:

$$\sqrt{8\pi/3}R^1_{eg}\equiv\langle e|V_q|g\rangle=\left[\frac{(J_e+e)(J_e+e-1)}{2J_e(2J_e-1)}\right]^{1/2},\qquad \Delta J=1,$$

$$\sqrt{8\pi/3}R^0_{eg}\equiv\langle e|V_q|g\rangle=\left[\frac{2(J_e-e)(J_e+e)}{2J_e(2J_e-1)}\right]^{1/2},\qquad \Delta J=1,$$

$$\sqrt{8\pi/3}R^{-1}_{eg}\equiv\langle e|V_q|g\rangle=\left[\frac{(J_e-e)(J_e-e-1)}{2J_e(2J_e-1)}\right]^{1/2},\qquad \Delta J=1,$$

$$\sqrt{8\pi/3}R^1_{eg}\equiv\langle e|V_q|g\rangle=-\left[\frac{(J_e+e)(J_e-e+1)}{2J_e(J_e+1)}\right]^{1/2},\qquad \Delta J=0,$$

$$\sqrt{8\pi/3}R^0_{eg}\equiv\langle e|V_q|g\rangle=\frac{\sqrt{2}e}{[2J_e(J_e+1)]^{1/2}},\qquad \Delta J=0,$$

$$\sqrt{8\pi/3}R^{-1}_{eg}\equiv\langle e|V_q|g\rangle=\left[\frac{(J_e-e)(J_e+e+1)}{2J_e(J_e+1)}\right]^{1/2},\qquad \Delta J=0,$$

$$\sqrt{8\pi/3}R^1_{eg}\equiv\langle e|V_q|g\rangle=\left[\frac{(J_e-e+1)(J_e-e+2)}{2(J_e+1)(2J_e+3)}\right]^{1/2},\qquad \Delta J=-1,$$

$$\sqrt{8\pi/3}R^0_{eg}\equiv\langle e|V_q|g\rangle=-\left[\frac{2(J_e-e+1)(J_e+e+1)}{2(J_e+1)(2J_e+3)}\right]^{1/2},\qquad \Delta J=-1,$$

$$\sqrt{8\pi/3}R^{-1}_{eg}\equiv\langle e|V_q|g\rangle=\left[\frac{(J_e+e+1)(J_e+e+2)}{2(J_e+1)(2J_e+3)}\right]^{1/2},\qquad \Delta J=-1,$$

where $q\equiv e-g=0$, ±1 and $\Delta J\equiv J_e-J_g=0$, ±1 (e.g. Condon & Shortley 1951). Note that these matrix elements are all real. They are normalized so that

$$\sum_{\alpha g}\int\mathrm{d}\Omega\,|M_{eg}(\boldsymbol{e}_\alpha)|^2=\sum_{\alpha g}R^q_{eg}R^{*q'}_{e'g}\int\mathrm{d}\Omega\,S_{\alpha q}S^*_{\alpha'q'} \tag{2.7}$$

$$=\frac{8\pi}{3}\sum_g R^q_{eg}R^{*q}_{eg}=1.$$

For generality, we should describe the ground and excited states using a density matrix. As long as the probability that a given ion is in an excited state is small, we can normalize the ground-state density matrix by

$$\rho_{gg'}=\frac{c_g c_{g'}^*}{c_{g''}c_{g''}^*}. \tag{2.8}$$

We normalize the excited state to the ground state so that $c_e c_e^* \ll 1$ is the total probability that an ion is in an excited state.

Suppose that collisions equally populate the ground sublevels. We average over many ions to form the mean density matrix

$$\overline{\rho}_{gg'}=(2J_g+1)^{-1}\delta_{gg'}. \tag{2.9}$$

We are interested in the rate of stimulated excitation from the ground level. Let the total intensity be $I_{\nu\Omega}$. We describe the polarization by another density matrix normalized so that

$$P_{\alpha\alpha'}(\theta,\phi)=\frac{\tilde{E}_\alpha \tilde{E}_{\alpha'}^*}{\tilde{E}_{\alpha''}\tilde{E}_{\alpha''}^*}. \tag{2.10}$$

We now write

$$I_{\alpha\alpha'}=I_{\nu\Omega}P_{\alpha\alpha'}. \tag{2.11}$$

The photon occupation number in this state is

$$n=\frac{c^2 I_{\alpha\alpha'}}{h\nu^3}. \tag{2.12}$$

If we ignore the possibility of collisional de-excitation, then, after each excitation, there will be a spontaneous transition back to the ground state. (We also assume that the radiation field is sufficiently weak that stimulated emission can be ignored.) Using equation (2.1) we can derive an evolution equation for the rate of change of the excited state:

$$\frac{\mathrm{d}\overline{\rho}_{ee'}}{\mathrm{d}t}=A\int M_{eg}(\boldsymbol{e}_\alpha)\rho_{gg'}M_{e'g'}^*(\boldsymbol{e}_{\alpha'})\,n\,\mathrm{d}\Omega - A\rho_{ee'}. \tag{2.13}$$

Hence in a steady state

$$\rho_{ee'}=\frac{c^2}{h\nu^3}\int \mathrm{d}\Omega\, I_{\alpha\alpha'}M_{eg}(\boldsymbol{e}_\alpha)\rho_{gg'}M_{g'e'}(\boldsymbol{e}_{\alpha'}), \tag{2.14}$$

where we use the notation $M_{ge}=M_{eg}^*$.

We define the effective absorption coefficient $\mu_{\alpha\alpha'}$ for radiation in the polarization state $P_{\alpha\alpha'}$ by

$$\mu_{\alpha\alpha'}=n_{\mathrm{i}}A\frac{c^2}{\nu^2}\phi_\nu M_{eg}(\boldsymbol{e}_\alpha)\rho_{gg'}M_{g'e}(\boldsymbol{e}_{\alpha'}), \tag{2.15}$$

where $\phi_\nu=(\lambda/n_{\mathrm{i}})(\mathrm{d}n_{\mathrm{i}}/\mathrm{d}v_\parallel)$ is the normalized ion velocity profile (assumed isotropic), $v_\parallel$ is the velocity component along the incident photon direction and n_{i} is the total ion density. Note that we sum over all excited states. This absorption coefficient is that for a specific frequency in the line.

Now let us specialize to the case where the radiation field is axisymmetric in the z-direction. We need only consider parallel and perpendicular polarization (cf. Fig. 1). We also assume complete frequency redistribution. In other words, the probability of emission at a given frequency ν is independent of the frequency of the absorbed photon and is also described by ϕ_ν. The emissivity $j_{\alpha\alpha'}$ per steradian is then given by

$$j_{\alpha\alpha'}=n_{\mathrm{i}}\phi_\nu A h\nu M_{ge}(\boldsymbol{e}_\alpha)\rho_{ee'}M_{e'g}(\boldsymbol{e}_{\alpha'}). \tag{2.16}$$

The equation of radiative transfer for the parallel component is then

$$\frac{\mathrm{d}I_\parallel}{\mathrm{d}s}=-\mu_\parallel I_\parallel + j_\parallel, \tag{2.17}$$

and similarly for the orthogonal polarization. It is more convenient to define a source function

$$S_{\parallel,\perp}=\frac{j_{\parallel,\perp}}{\mu_{\parallel,\perp}}=\frac{h\nu^3}{c^2}\left[\frac{M_{ge}(\boldsymbol{e}_{\parallel,\perp})\rho_{ee'}M_{e'g}(\boldsymbol{e}_{\parallel,\perp})}{M_{eg}(\boldsymbol{e}_{\parallel,\perp})\rho_{gg'}M_{g'e}(\boldsymbol{e}_{\parallel,\perp})}\right]. \tag{2.18}$$

There is a complication that must be considered when the incident radiation is arbitrarily polarized. A substance that is capable of efficient absorption must also be dispersive. This implies that photons propagating between collisions must be resolved into the eigenstates of propagation, and there may be a phase difference introduced by the propagation. In this paper, we shall restrict attention to simple geometries where there will be no such 'propagation coupling' between different polarization states.

We now assume a fixed radiation field. The simplest example is the case of the unidirectional radiation field represented by

$$I(\theta,\phi)\propto\delta(\mu-1). \tag{2.19}$$

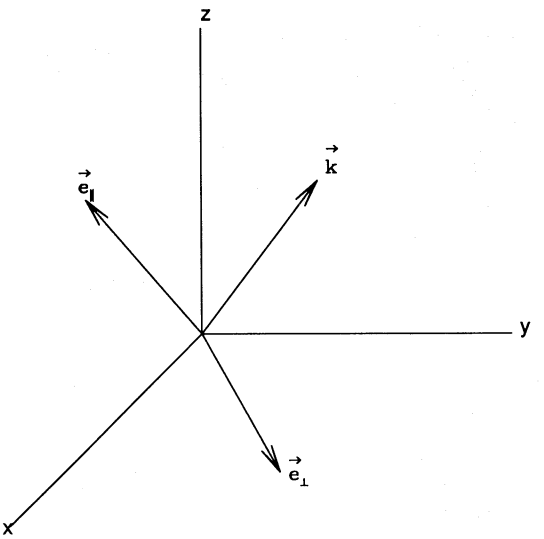

Figure 1. The basis vectors of the photon states. $\boldsymbol{e}_\parallel$ lies in the $\boldsymbol{k}$–$\hat{\boldsymbol{z}}$ plane, where $\boldsymbol{k}$ is the vector of the photon, and $\boldsymbol{e}_\perp$ is in the $\hat{\boldsymbol{x}}$–$\hat{\boldsymbol{y}}$ plane.

When the beam propagates along the z-axis, there can only be upwards transitions with $\Delta M = \pm 1$. This is the key process. The direct substitution of equation (2.19) into equation (2.14) gives

$$\rho_{ee'} \propto \delta_{ee'}[J_e(J_e-1)+e^2], \qquad \Delta J = 1, \tag{2.20a}$$

$$\rho_{ee'} \propto \delta_{ee'}[J_e(J_e+1)+e^2], \qquad \Delta J = 0, \tag{2.20b}$$

$$\rho_{ee'} \propto \delta_{ee'}[(J_e+1)(J_e+2)+e^2], \qquad \Delta J = -1. \tag{2.20c}$$

The net polarization for emission at right angles, P_0, is given by

$$P_0 = \frac{j_\parallel(0) - j_\perp(0)}{j_\parallel(0) + j_\perp(0)}, \tag{2.21}$$

where $j_{\parallel,\perp}(0) = j_{\parallel,\perp}(\mu = 0, \phi)$. By combining equations (2.20a,b,c) and equation (2.16) and substituting them into equation (2.21), we obtain

$$P_0 = \frac{(J_e+1)(2J_e+3)}{(26J_e^2 - 15J_e - 1)}, \qquad \Delta J = 1, \tag{2.22a}$$

$$P_0 = \frac{(2J_e-1)(2J_e+3)}{(12J_e^2 + 12J_e + 1)}, \qquad \Delta J = 0, \tag{2.22b}$$

$$P_0 = \frac{J_e(2J_e-1)}{(26J_e^2 + 67J_e + 40)}, \qquad \Delta J = -1. \tag{2.22c}$$

In Table 1 P_0 is shown for the cases $J_e = 1, 2, 3, 4, 5$ and ∞, for all the possible transitions $\Delta J = \pm 1, 0$. Note that a $0 \rightarrow 1$ transition with a beam pattern of classical electron scattering produces 100 per cent polarization when viewed from a perpendicular direction (e.g. Hamilton 1947; Webster 1986).

The polarization for emission at an arbitrary angle P_μ can be calculated by considering the intensity contributions for each polarization given by

$$\Delta I_\perp \propto j_\perp(0), \qquad \Delta I_\parallel \propto j_\parallel(0)\sin^2\theta + j_\perp(0)\cos^2\theta, \tag{2.23}$$

and

$$P_\mu = \frac{\Delta I_\parallel - \Delta I_\perp}{\Delta I_\parallel + \Delta I_\perp} = \frac{P_0 \sin^2\theta}{1 + P_0\cos^2\theta}. \tag{2.24}$$

An isotropic radiation field naturally produces no polarization, as may be quickly demonstrated. The same is true for a $P_1(\mu)$ variation ($\mu = \cos\theta$). We therefore adopt a variation $I(\mu) \propto \mu^2$. Lower spherical harmonic components can be added to this without changing the polarized flux. We use the rate equations to solve for the density matrix of the excited state for a variety of transitions. We can then compute the absorption cross-section and emissivity as a function of μ for the two polarization states. The results are shown in Fig. 2.

As the ground sublevels are equally populated, the absorption coefficient is independent of the polarization. The source function is unpolarized when the observer lies along the z-axis (the symmetry axis). What is rather surprising is that the source function is undetectably small for transitions with $J_e = J_g - 1$. For most common resonance transitions with $\Delta J = 1$, the source function is strongly polarizing. The maximum value of $S_\perp/S_\parallel$ is 2 for a $0 \rightarrow 1$ transition (e.g. C III λ977).

3 EMISSION AND ABSORPTION COEFFICIENTS – RADIATIVE MIXING

When the collision rate is sufficiently low relative to the radiative excitation rate, it is no longer assured that the ground sublevels will be equally populated (e.g. Varshalovich 1965).

The electron collision rate C is given by

$$C = n_e \int_0^\infty v\sigma f(v)\,dv \sim 6\times 10^2\ \mathrm{s}^{-1}, \tag{3.1}$$

where $f(v)$ is the Maxwellian velocity distribution, n_e is the electron density, and σ is the collision cross-section. Here we use the relation $\sigma \sim 10^{-15}\ \Omega/\omega\ \mathrm{cm}^2$, which is valid at a typical temperature of 10^4 K, where Ω is the effective collision strength and ω is the statistical weight (e.g. Osterbrock 1989). For many broad lines the values of the effective collision strength have been collected by Osterbrock & Wallace (1977), typical values being 1–20 dependent on the ion species and the temperature. For order-of-magnitude calculations, we adopt $\Omega/\omega \sim 1$.

The radiative excitation rate R is given by

$$R = \int d\nu n_\nu \sigma_\nu c \sim \frac{\pi e^2}{mc} f_{\mathrm{abs}} n_{\nu 0} c \sim (8.0\times 10^8\ \mathrm{cm^3\ s^{-2}})\, f_{\mathrm{abs}} n_{\nu 0}, \tag{3.2}$$

Table 1. Polarization scattered perpendicular to a beam of radiation.

$\Delta J \backslash J_e$	0	$\frac{1}{2}$	1	$\frac{3}{2}$	2	$\frac{5}{2}$	3	$J_e = \infty$
1	–	–	1.000	0.429	0.288	0.226	0.191	0.077
0	–	0	0.200	0.261	0.288	0.302	0.310	0.333
−1	0	0	0.008	0.015	0.022	0.029	0.032	0.077

$\Delta J = J_e - J_g$. The polarization is for unidirectional radiation distribution in the collisional mixing case. No electric dipole transitions are allowed for $J_e = 0$ for $\Delta J = 0, 1$.

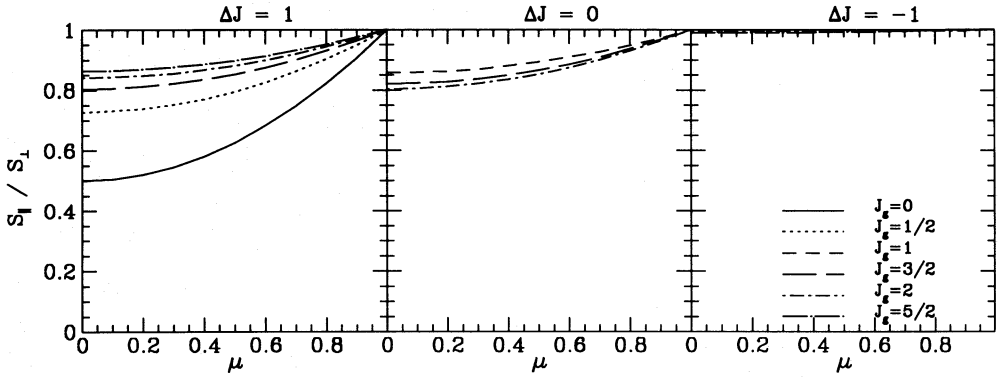

Figure 2. The ratio of parallel and perpendicular source functions for the collisional mixing case with an unpolarized radiation field $I_{aa'} \propto \mu^2 \delta_{aa'}$. J_g is the total angular momentum of the ground state and $J_e = J_g + \Delta J$ is that of the excited state. As the ground sublevels are equally populated, the absorption coefficient is independent of the polarization and so the source function behaves like the emissivity. Source functions for permitted values of J_g are plotted where the curves are distinguishable. Different ground states are represented by different line styles.

where n_ν is the photon density per unit frequency range, ν_0 is the resonance frequency, σ_ν is the scattering cross-section at frequency ν and $f_{\rm abs}$ is the oscillator strength associated with the photon absorption.

The ionization parameter U is defined as the ratio of the H-ionizing photon density n_γ to the free electron density $n_{\rm e}$, i.e.

$$U \equiv \frac{n_\gamma}{n_{\rm e}}. \tag{3.3}$$

Suppose that we have a power spectrum of photon density given by

$$n_\nu \propto \nu^{-3/2}. \tag{3.4}$$

Then

$$\begin{aligned} n_\gamma &= \int_{\nu_{\rm th}}^{\infty} n_\nu(\nu_{\rm th}) \left(\frac{\nu}{\nu_{\rm th}}\right)^{-3/2} {\rm d}\nu \\ &= 2 n_\nu(\nu_{\rm th})\, \nu_{\rm th}, \end{aligned} \tag{3.5}$$

where $\nu_{\rm th}$ is the threshold frequency for H ionization. Hence

$$\begin{aligned} n_{\nu 0} = n_\nu(\nu_0) &= \frac{n_\gamma}{2\nu_{\rm th}} \left(\frac{\nu_0}{\nu_{\rm th}}\right)^{-3/2} \\ &= U n_{\rm e} \frac{\nu_{\rm th}^{1/2}}{\nu_0^{3/2}}. \end{aligned} \tag{3.6}$$

Hence the radiative excitation rate R is given in terms of U:

$$R \sim 1.5 \times 10^4 f_{\rm abs} U n_{\rm e10} \nu_{15}^{-3/2}, \tag{3.7}$$

where $\nu_{15} = \nu_0 / 10^{15}\ {\rm s}^{-1}$, and finally

$$C/R \sim 4 \times 10^{-2} T_4^{1/2} U^{-1} \nu_{15}^{3/2} f_{\rm abs}^{-1}. \tag{3.8}$$

Given the ionization parameter $U \sim 10^{-1}$, most permitted lines that have $f_{\rm abs} \sim 1$ satisfy the radiative mixing condition $C/R \ll 1$. Many permitted lines are multiplets and they are not, in general, resolved in the broad-line region of AGN where the typical velocity $\sim 10^4$ km s^{-1} exceeds the width that separates the multiplets. We defer the detailed model calculations of the polarization of those lines to Paper III.

When the radiative excitations dominate, we can derive an evolution equation for the ground level, again ignoring stimulated emission. In a steady state,

$$\begin{aligned} \frac{{\rm d}\overline{\rho}_{gg'}}{{\rm d}t} &= A \int {\rm d}\Omega\, M_{ge}(\boldsymbol{e}_a) \overline{\rho}_{ee'} M_{e'g'}(\boldsymbol{e}_a) \\ &\quad - \frac{c^2 A}{h\nu^3} \int {\rm d}\Omega\, I_{aa'} M_{eg}(\boldsymbol{e}_a) \rho_{gg'} M_{g'e}(\boldsymbol{e}_{a'}) \\ &= 0, \end{aligned} \tag{3.9}$$

where no summation is assumed over g and g' in the second term. This equation was combined with equation (2.14), and an iterative solution for $\rho_{gg'}$, $\rho_{ee'}$ was derived. Equations (2.15) and (2.18) were then used to derive absorption coefficients and source functions for the radiative mixing case.

We have carried out this procedure for the same transitions investigated in the preceding section, adopting a similar radiation field. Our results are displayed in Figs 3 and 4. For transitions with angular momenta $J > 1$, the radiative mixing enhances the polarization. In Fig. 4, the absorption coefficients vary with μ, which contrasts with the result for collisional mixing where the absorption coefficients are isotropic and polarization-independent. With the beam-like radiation distribution, the net effect of the radiative mixing is to overpopulate sublevels with higher $|g|$ for transitions of $\Delta J = 1$ and sublevels with lower $|g|$ for transitions of $\Delta J = 0, -1$. $\mu_\parallel / \mu_\perp$ is maximized for the transition $1 \rightarrow 0$ on account of the enhanced population in the $g = 0$ state. In the case $\Delta J = 1$, the emissivity ratio $j_\parallel / j_\perp$ is maximized at large angular momenta because of the overpopulation in the $e = 0$ state. The absorption coefficient is almost independent of polarization and so the source function behaves like the emissivity. The radiative mixing has no effect on the transitions with $J_g \leq 1/2$, and therefore we obtain the same source functions and absorption coefficients as in the case of collisional mixing.

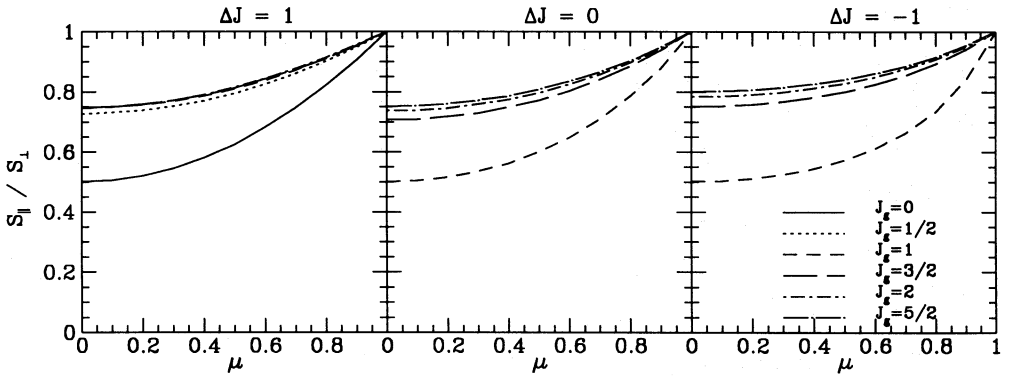

Figure 3. The ratio of source functions for the radiative mixing case, with the same conditions as described for Fig. 2.

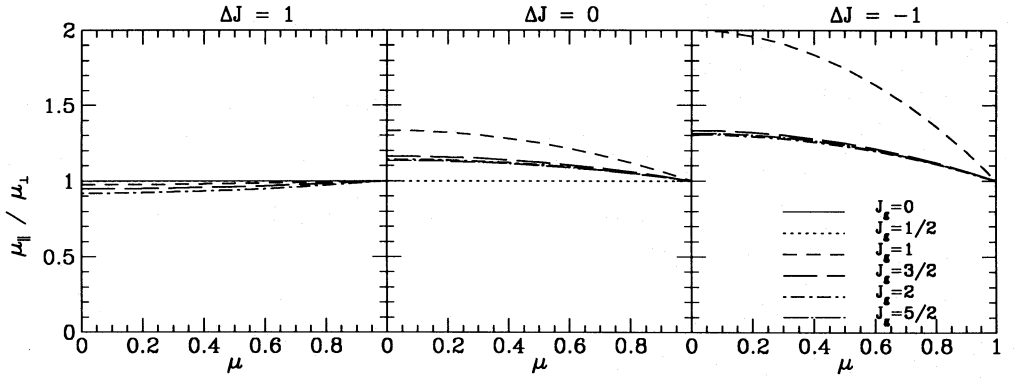

Figure 4. The ratio of the parallel component of the absorption coefficient $\mu_{\parallel}$ to the perpendicular component $\mu_{\perp}$ for the radiative mixing case, with the same radiation field as in Fig. 2.

Fig. 5 shows that a notable change in the emissivity occurs for transitions associated with large angular momenta, but nevertheless the largest polarization is expected in the permitted lines for the transition $1 \rightarrow 0$ or $1 \rightarrow 1$.

4 EMISSION AND ABSORPTION COEFFICIENTS – MAGNETIC MIXING

There is an additional complication that may be present in a broad-emission-line cloud in an AGN, namely a magnetic field. Magnetic fields of strength $B \gtrsim 1$ G have been invoked in models by Rees (1987) and Emmering et al. (1992) in order to account for cloud confinement in such a way that the magnetic stress is comparable with the gas pressure in the emission-line clouds. The associated electron–cyclotron frequencies $\nu_L \sim 3(B/1\,\mathrm{G})$ MHz can then exceed the radiative excitation rate so that the ground sublevels can be further repopulated. Magnetic mixing has no influence in the collision-dominated case as the ground sublevels are already equally populated and the Zeeman splitting energy is small compared with the Doppler linewidth. Magnetic mixing may also be relevant for the excited-state density matrix for semi-forbidden transitions with Einstein A coefficients in the range ~1–100 Hz. We consider these two possibilities in turn.

Suppose that an individual ion is prepared in a ground state with a density matrix $\rho_{gg'}$. If the Hamiltonian is denoted H, the state will evolve according to

$$i\hbar \frac{d\rho_{gg'}}{dt} = [H, \rho_{gg'}] \tag{4.1}$$

(e.g. Merzbacher 1961). In other words, the condition for the density matrix to remain unchanged is that it commute with the Hamiltonian. The effect of a magnetic field will be to break the degeneracy of the ground sublevels. Let us expand the density matrix in the basis eigenstates of the magnetic perturbation. The off-diagonal elements of the density matrix will evolve and mix at a rate comparable with the Zeeman splitting frequency between the various states. If several periods of this relative precession can occur between excitations (i.e. $\nu_L \gg R$, where R is the radiative excitation rate), the off-diagonal elements of the mean density matrix will average to zero. The diagonal elements will, by contrast, be unaffected. We therefore treat the strong magnetic mixing limit by expanding the radiation field in eigenstates referred to the magnetic field direction and ignoring all the off-diagonal matrix elements $\rho_{gg'}$. Clearly, this makes no difference when the radiation field is axisymmetric with respect to the magnetic field. When this symmetry is broken,

however, different source functions and absorption coefficients will result.

We now present an illustrative problem in which the radiation field is unpolarized and has a P_2 angular distribution with respect to a symmetry direction oriented perpendicular to the magnetic field. The magnetically modified source functions and absorption cross-sections are displayed in Figs 6 and 7 respectively. We find that the polarization pattern is similar to the radiative mixing case for the transitions $\Delta J = 1$ only, and that the direction of the polarization is reversed in the case $\Delta J = -1$ compared to the case without a magnetic field. The behaviour of interest occurs in the transitions $\Delta J = 0$, where the polarization direction changes as μ increases from 0 to 1. The magnetic field breaks the azimuthal symmetry and hence we should no longer expect polarization to be 0 at $\mu = 1$. In particular, the largest degree of

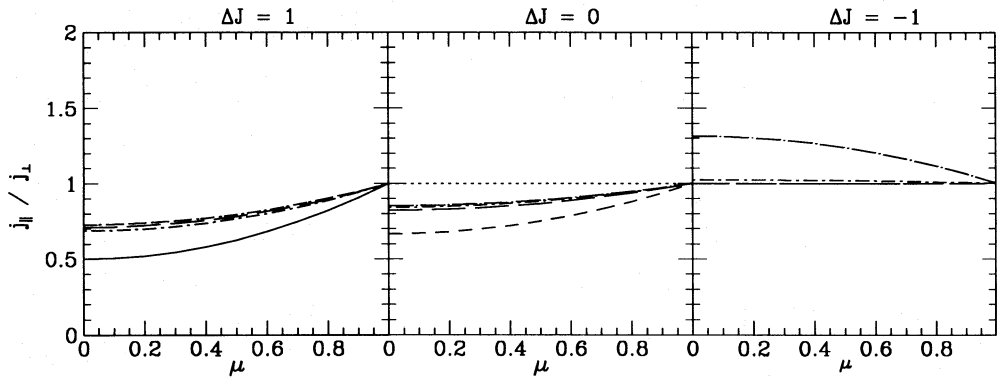

Figure 5. The ratio of emissivities for the radiative mixing case.

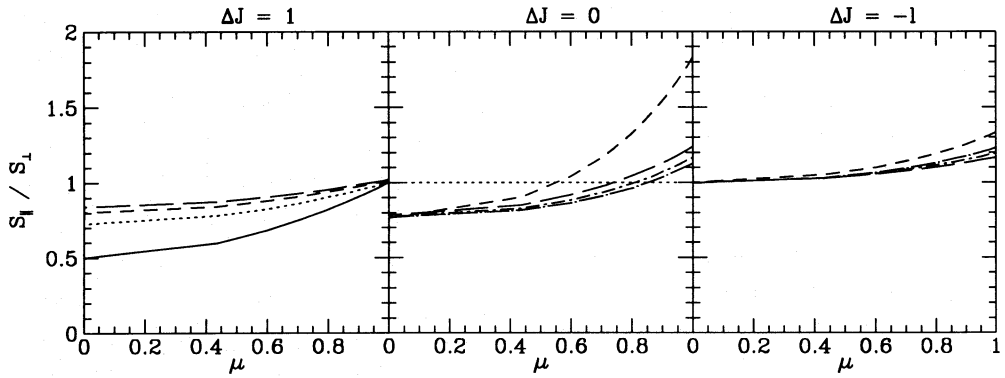

Figure 6. The ratio of source functions for the magnetic mixing case. The conditions are as described in Fig. 2 with the addition of a magnetic field along the x-axis, and the absorption and emission coefficients are calculated as a function of $\mu = \cos\theta$, where θ is the angle between the z-axis (the symmetry axis) and the line of sight, keeping $\phi = 0$. The lines represent the same values of J_g as in Fig. 2.

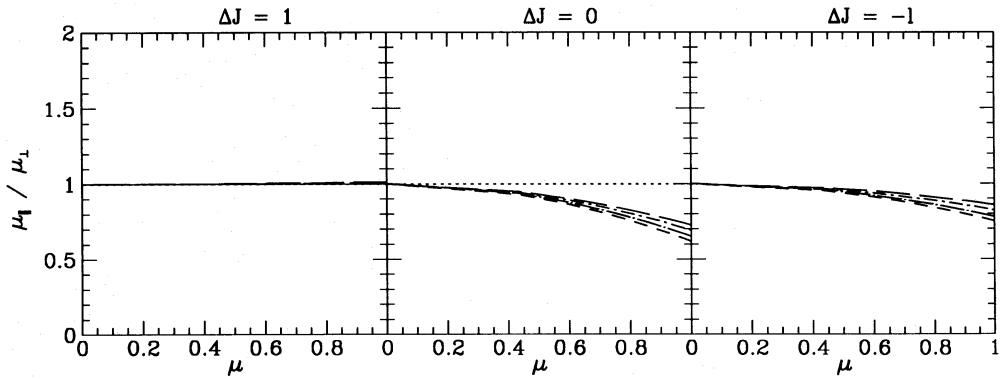

Figure 7. The ratio of absorption coefficients for the magnetic mixing case for different transitions. The lines represent the same values of J_g as in Fig. 2.

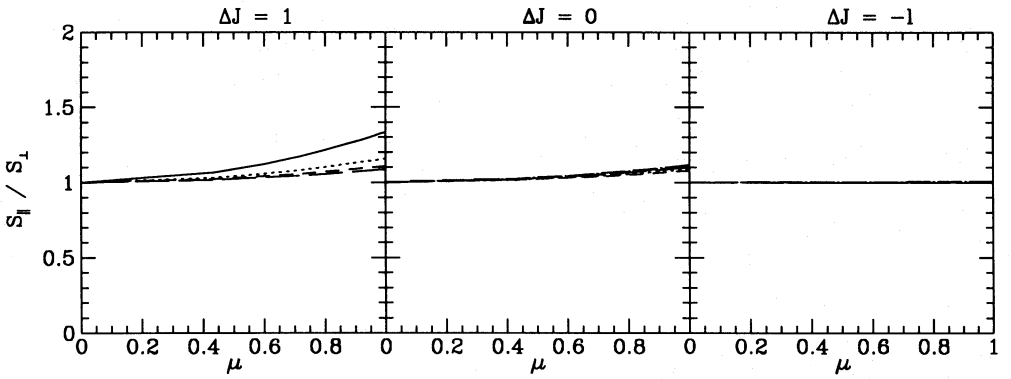

Figure 8. The ratio of source functions for the magnetic mixing case applied to semiforbidden lines with the same conditions as described in Fig. 6. See Fig. 2 for the values of J_g represented by the different line types

polarization is seen at $\mu = 1$ in the transitions $\Delta J = -1$. As explained in the previous section, the transitions with $J_g \leq 1/2$ again show the same result as we have obtained in the collisional mixing case without a magnetic field.

For comparison, we have also considered what happens to the same types of transition when the excited states are magnetically mixed by the same radiation field (cf. Fig. 8), while the ground states are collisionally mixed and have uniform occupancy. In this case, the degree of polarization is lower than that in the collisional mixing case without a magnetic field. The maximum polarization in the magnetic mixing case is 14 per cent at $\mu = 1$, as opposed to 33 per cent at $\mu = 0$ without magnetic mixing. It is also notable that the polarization increases from zero as μ increases, which clearly shows that the azimuthal symmetry is broken by the magnetic field.

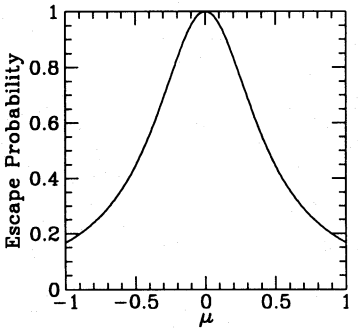

Figure 9. The polarization-independent anisotropic escape probability adopted for the purpose of the simple calculation suitable for the geometry of cylindrical clouds and given by the analytic formula $\lambda = 1/(1 + k\mu^2)$, with $k = 5$.

5 ANISOTROPIC ESCAPE PROBABILITY

In the examples we have considered so far, the radiation field is considered fixed and we have computed the source functions and absorption coefficients. As a final illustration, we show how to compute the emergent polarization when we define an anisotropic, although polarization- and frequency-independent, escape probability. We suppose, for simplicity, that the line photons are *created* isotropically at a rate of S_0 per steradian. (As we shall describe in subsequent papers, more complex conditions can arise in the emission-line clouds, although the principles are unaffected.) The radiation field will evolve on an escape time-scale, which is typically much longer than the time it takes the ions to establish radiative equilibrium. The radiation field will relax to a steady state, satisfying

$$(\lambda_{aa'} + \eta_{aa'}) I_{aa'} = S_0 \delta_{aa'} + j_{aa'} \tag{5.1}$$

subject to the photon-conservation condition

$$\int d\Omega \eta_{aa'} I_{aa'} = \int d\Omega j_{aa'}. \tag{5.2}$$

We now suppose for illustration that the escape probability is anisotropic so that a photon emitted with a direction cosine μ with respect to the symmetry axis has an escape probability (independent of polarization and location)

$$\lambda_{aa'}(\mu) = (1 + k\mu^2)^{-1} \delta_{aa'}, \tag{5.3}$$

where k is the anisotropy parameter. The effective optical depth is measured by one adjustable parameter which can be chosen to be the ratio

$$r = \int d\Omega (S_{0\parallel} + S_{0\perp}) \Big/ \int d\Omega (j_\parallel + j_\perp). \tag{5.4}$$

The emergent polarization along a given direction is then a function of k and r. Note that, if we were to ignore the scattering, then a P_2 anisotropic radiation field would be established.

We have solved equation (5.1) iteratively, for the radiative mixing case, updating the ground-state density matrix at each iteration. We find that ~30 iterations are sufficient to achieve convergence, depending on R. The angular distribution of the degree of polarization of the escaping radiation

$$P(\mu) = \frac{I_\parallel - I_\perp}{I_\parallel + I_\perp} \tag{5.5}$$

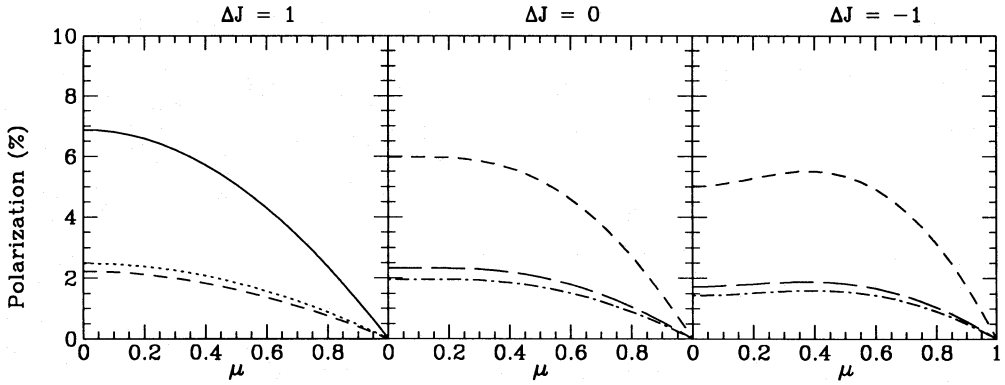

Figure 10. The polarization from the anisotropic escape probability given in Fig. 9. We choose the ratio of scattered photons to created photons $r = \int d\Omega (j_{\parallel} + j_{\perp}) / \int d\Omega (S_{0\parallel} + S_{0\perp}) = 4$, and the polarization P is given by $P = (I_{\parallel} - I_{\perp})/(I_{\parallel} + I_{\perp})$. See Fig. 2 for the values of J_g represented by the different lines.

is shown in Fig. 10 for $k = 5$, $r = 4$. A degree of polarization higher than 6 per cent can be achieved for the transitions $J_g = 0 \rightarrow J_e = 1$, $J_g = 1 \rightarrow J_e = 1$ and $J_g = 1 \rightarrow J_e = 0$. For $\Delta J = 1$, there is a clear maximum in the polarization at $\mu = 0$. For $\Delta J = 0$, the polarization is roughly constant for $\mu \lesssim 0.5$, and for $\Delta J = -1$ maximum polarization is seen at $\mu \sim 0.4$. Again, small J_g is conducive to high polarization. Similar results are found for $r > 1$. Although this example is artificial, it does demonstrate that a true estimate of the emergent polarization requires that we solve the complete radiative transfer equations.

6 CONCLUSION

In this paper we have analysed some of the physical effects that might be important in establishing the linear polarization of AGN emission lines. We have computed the polarization dependence of the emission and absorption coefficients in a variety of radiation fields. We have demonstrated that polarization requires there to be an anisotropic radiation field.

In estimating the magnitude of the polarization, we have essentially treated the photons in the Markov approximation. That is to say, we have computed the absorption and emission probabilities assuming that the radiation field is independent of the photon frequency, which in turn depends upon the past history. This is essentially the hypothesis of complete redistribution, which, as we shall argue in Paper II, is a poor approximation for polarization calculations as the escaping photons in the wings of the line are significantly more anisotropic than those in the core.

ACKNOWLEDGMENTS

We thank M. Cohen, R. Emmering, R. Goodrich and J. Miller for helpful discussions. We are very grateful to G. M. Voit for his friendly comments and advice. Support under NASA grant NAGW2372 and NSF grant AST89-17765 is gratefully acknowledged.

REFERENCES

Condon E. U., Shortley G. H., 1951, The Theory of Atomic Spectra. Cambridge Univ. Press, Cambridge
Emmering R. T., Blandford R. D., Shlosman I., 1992, ApJ, 385, 460
Goodrich R. W., 1991, PASP, 103, 1314
Hamilton D. R., 1947, ApJ, 106, 457
Merzbacher E., 1961, Quantum Mechanics. Wiley, New York
Netzer H., 1990, Active Galactic Nuclei. Springer-Verlag, Berlin
Osterbrock D. E., 1989, Astrophysics of Gaseous Nebulae and Active Galactic Nuclei. University Science Books, Mill Valley, CA
Osterbrock D. E., Wallace R. K., 1977, Astrophys. Lett., 19, 11
Rees M. J., 1987, MNRAS, 228, 47P
Varshalovich D. A., 1965, SvA, 9, 442
Webster A., 1986, MNRAS, 217, 761